



# CHORUS

This is the accepted manuscript made available via CHORUS. The article has been published as:

## Inter-Landau-level Andreev Reflection at the Dirac Point in a Graphene Quantum Hall State Coupled to a NbSe<sub>2</sub> Superconductor

Manas Ranjan Sahu, Xin Liu, Arup Kumar Paul, Sourin Das, Pratap Raychaudhuri, J. K. Jain, and Anindya Das

Phys. Rev. Lett. **121**, 086809 — Published 24 August 2018

DOI: [10.1103/PhysRevLett.121.086809](https://doi.org/10.1103/PhysRevLett.121.086809)

# Inter Landau level Andreev reflection at the Dirac point in graphene quantum Hall state coupled to NbSe<sub>2</sub> superconductor

Manas Ranjan Sahu,<sup>1</sup> Xin Liu,<sup>2</sup> Arup Kumar Paul,<sup>1</sup> Sourin Das,<sup>3</sup> Pratap Raychaudhuri,<sup>4</sup> J. K. Jain,<sup>5</sup> and Anindya Das<sup>1,\*</sup>

<sup>1</sup>*Department of Physics, Indian Institute of Science, Bangalore 560012, India*

<sup>2</sup>*School of Physics, Huazhong University of Science and Technology, Wuhan 430074, China*

<sup>3</sup>*Indian Institute of Science Education and Research, Kolkata, Mohanpur 741246, India*

<sup>4</sup>*Tata Institute of Fundamental Research, Homi Bhabha Road, Colaba, Mumbai 400 005, India*

<sup>5</sup>*Department of Physics, The Pennsylvania State University, University Park, Pennsylvania 16802, USA*

Superconductivity and quantum Hall effect are distinct states of matter occurring in apparently incompatible physical conditions. Recent theoretical developments suggest that the coupling of quantum Hall effect with a superconductor can provide a fertile ground for realizing exotic topological excitations such as non-abelian Majorana fermions or Fibonacci particles. As a step toward that goal, we report observation of Andreev reflection at the junction of a quantum Hall edge state in a single layer graphene and a quasi-two dimensional niobium diselenide (NbSe<sub>2</sub>) superconductor. Our principal finding is the observation of an anomalous finite-temperature conductance peak located precisely at the Dirac point providing a definitive evidence for inter-Landau level Andreev reflection in a quantum Hall system. Our observations are well supported by detailed numerical simulations, which offer additional insight into the role of the edge states in Andreev physics. This study paves the way for investigating analogous Andreev reflection in a fractional quantum Hall system coupled to a superconductor to realize exotic quasiparticles.

Proximity effect through Andreev reflection (AR) is the primary ingredient for engineering a topological superconductor, which is expected to be a breeding ground for new types of topological excitations[1–8]. Discovery of graphene in the last decade[9], aided by developments in improving device quality by encapsulating with hexagonal Boron Nitride[10, 11] (hBN), provides one of the best opportunities to extend the study of AR for Dirac electrons in proximity to superconductor[12–19]. In these systems an incident electron from the single layer graphene (SLG) with a finite excitation energy combines with another electron below the Fermi energy ( $E_F$ ) to form a Cooper pair at the junction (Fig. 1a-top). The AR and its transition from retro to non-retro reflection has been observed [17]. More interestingly, when  $E_F$  is aligned with the Dirac point, AR requires an inter-band process and is predicted to be specular (Fig. 1a-top), as observed recently in bilayer graphene[16].

Exotic physics is predicted to arise from the coupling between a superconductor and a topological quantum Hall (QH) state. In particular, this system has been proposed as a novel route for creating a variety of non-abelian anyons, which have been hailed as possible building blocks for future topological quantum computation[6, 20, 21]. The physics of AR is predicted to alter dramatically in the QH regime [22–24], where electron transport occurs primarily through the chiral edge states, which themselves are topologically robust manifestations of the Landau Levels (LLs) in the interior of the sample. On the QH plateau, an incident chiral electron is expected to bounce back as an Andreev-reflected chiral hole propagating in the same direction as the incoming electron (Fig. 1a - bottom)[25], due to the sign

reversals of both the charge and the mass. A difficulty in experimentally investigating this physics is the fact that high magnetic fields required for the QH effect are inimical to superconductivity. Important progress has recently been made in this direction. Supercurrent and Josephson coupling in QH regime at SLG-superconductor interface have been demonstrated at relatively low magnetic field ( $\sim 2$ T)[26–28]. At high magnetic fields ( $\sim 10$ T) the superconducting correlations in QH edge has been realized recently[29].

In this work, we show that a coexistence of, and a coupling between, a QH system and a superconductor can be realized and studied in a system of SLG coupled to a NbSe<sub>2</sub> superconductor. Our results reveal that at high magnetic fields, when the breaking of the spin and valley symmetries generally fully splits the zeroth Landau level[30–32], AR manifests most strikingly through an anomalous conductance peak located precisely at the Dirac point (DP). We attribute this peak to inter-Landau level AR, and confirm its physical origin by detailed theoretical simulations.

Our devices consist of an SLG partially covered with a thin film of NbSe<sub>2</sub> (Fig. 1b). Details of the fabrication and measurement schemes are given in the Supplemental Material (SM)[33] Sec. SI1. We show results from three devices as a function of the back-gate voltage ( $V_{BG}$ ), the source-drain bias voltage ( $V_{SD}$ ), the temperature ( $T$ ) and the magnetic field ( $B$ ). The highest mobility of 60,000 cm<sup>2</sup>/V.sec was obtained in device-3, where the carrier inhomogeneity ( $\delta n$ ) due to charge puddles was  $\sim (3-5) \times 10^9$  cm<sup>-2</sup> which corresponds to Fermi energy broadening ( $\delta E_F$ ) of  $\sim 6-8$ meV [34]. The characterization of several devices is shown in SM Sec. SI1[33]. Fig. 1c presents the

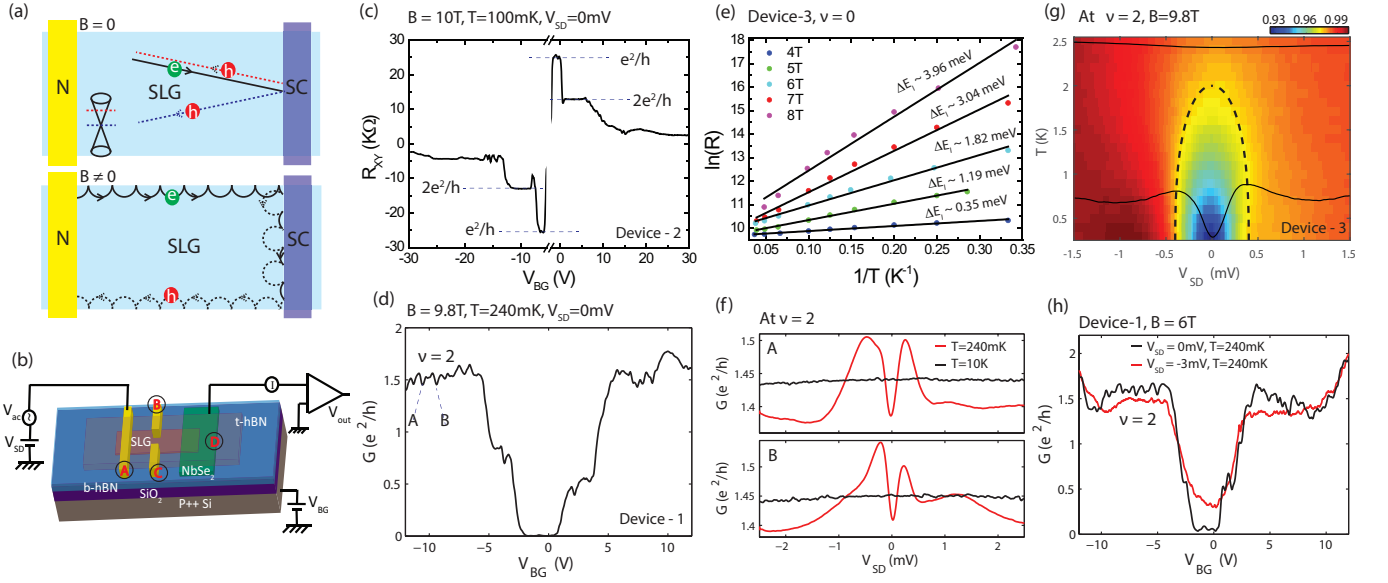


Figure 1. (Color Online) (a) (top) AR in graphene at  $B = 0$ . The red (blue) dashed line shows retro (specular) AR. (bottom) Classical picture of AR at the interface of QH edge state and superconductor based on skipping orbit. The electron and hole orbits have the same chirality for intra-band process. (b) Schematic of the experimental measurement setup of hBN protected graphene devices. For  $R_{xy}$  measurement current is injected between A and D, voltage is measured between C and D. For the two probe conductance measurement of the SLG-NbSe<sub>2</sub> junction voltage is applied at A, and current is measured at D. (c)  $R_{xy}$  of device 2 at  $B = 10T$  showing symmetry broken QH plateaus. (d) Two-terminal gate response of device 1 between Au-SLG-NbSe<sub>2</sub> at  $B = 9.8T$  and  $V_{SD} = 0mV$ . (e) Activation plot for device 3 at the Dirac point for different magnetic fields; the corresponding insulating gaps are shown on the figure. We note that the resistance changes by up to three orders of magnitude over the range of the fits. (f)  $dI/dV$  as a function of  $V_{SD}$  measured in device 1 at  $B = 9.8T$  on the  $\nu = 2$  LL at the positions A and B marked in fig(d); BCS peaks are present at 240 mK (red) but not at 10K (black). (g) 2D colormap of normalized  $dI/dV$  versus  $V_{SD}$  as a function of temperature at  $B = 9.8T$  for device 3. Superconductivity vanishes at around 2K. The black dashed line is the theoretical temperature dependence of BCS gap. The cut lines are shown at 240mK and 2.5K. (h) The gate responses of device 1 for 6T at  $V_{SD} = 0$  (black) and for  $V_{SD} > \Delta$  (red). The former has enhanced conductance.

Hall resistance,  $R_{xy}$ , of device 2 at  $B = 10T$ , where the plateaus at  $2e^2/h$  and  $1e^2/h$  are clearly visible. From the  $B$  dependence of Shubnikov de Haas oscillations[35, 36] the LL broadening of  $\Gamma \sim 4.5$  meV was obtained (SM Sec. SI3[33]). The two-probe conductance ( $G$ ) measured between SLG - superconductor contact at 10T is shown in Fig. 1d (device 1). The value of conductance on the plateaus is lower than the ideal value due to the contact resistance of  $\sim 1.5$  kilo-ohms at the SLG - NbSe<sub>2</sub> junction. In addition to different broken symmetries, an insulating state, i.e. a  $\nu = 0$  plateau, is observed at the DP as previously reported in the literature [37–41]. Using thermally activated carrier transport model we have determined the insulating gap of the  $\nu = 0$  plateau (SM Sec. SI5[33]). Previous studies[40, 41] have reported that the value of insulating gap of  $\nu = 0$  plateau depends on  $\Gamma$ , and the measured activation gap is nothing but the mobility gap,  $\Delta E_I = \Delta E_{LL} - \Gamma$ [36, 42]. At 10T,  $\Delta E_I \sim 5$  meV was measured for device 3 (SM sec. SI5[33]), and activation plots at several  $B$  are shown in Fig. 1e. The details of the activation plots of device 1 and device 2 are shown in SM Sec. SI5[33].

We begin by demonstrating that superconductivity

in NbSe<sub>2</sub> survives up to high perpendicular magnetic fields where the uncovered graphene is comfortably in the QH regime. Fig. 1f shows the differential conductance ( $dI/dV$ ) as a function of  $V_{SD}$ , called the Andreev curve, for the values of  $V_{BG}$  marked A and B in Fig. 1d on the  $\nu=2$  plateau. The existence of superconductivity is evident from the BCS like conductance peaks at about  $\pm 0.5$  meV for device 1 at  $B = 9.8T$ . Similar features are observed for device 2 (SM Fig. SI4-5f and Sec. SI6[33]). Bias spectroscopy (SM Sec. SI6[33]) allows us to extract the low-T superconducting gap ( $2\Delta$ ) as a function of magnetic field, which we show in Fig. 4a; the large error bars arise primarily due to the asymmetric nature of the Andreev curve (the possible origin of which is discussed in more detail below). The superconducting gap of NbSe<sub>2</sub> flake,  $2\Delta \sim 2meV$  and  $T_C \sim 7K$  at 0T was directly characterized in our previous work (Fig. 3a of ref[17]), which is consistent with the 0T data in Fig. 4a. Fig. 1g shows the temperature dependence of the Andreev curves at  $B=9.8T$ , which produces a  $T_c \sim 2K$  where the BCS peaks disappear. We can relate the  $T_c$  to superconducting gap through  $2\Delta = 4.07k_B T_c \sim 0.7meV$  (the factor 4.07 was determined in Ref. [43] for NbSe<sub>2</sub>),

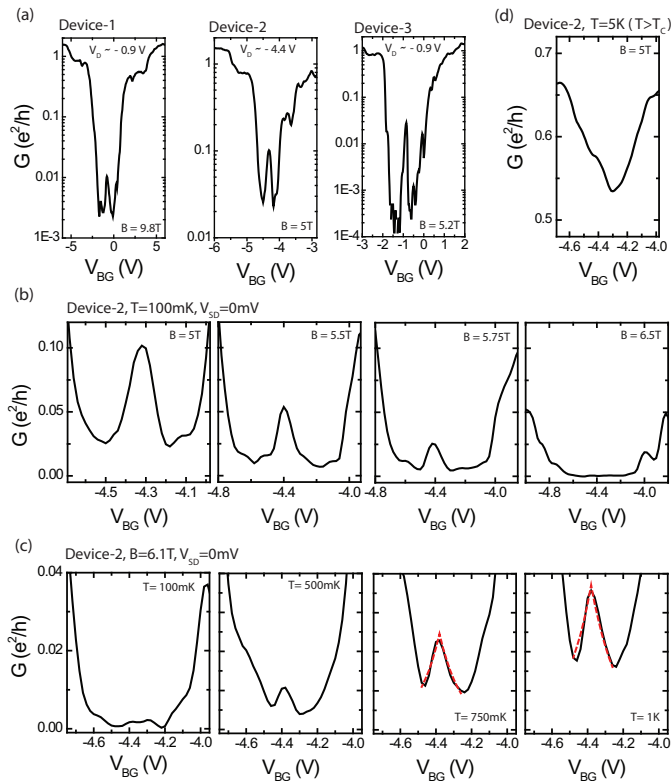


Figure 2. (Color Online) (a) The anomalous conductance peak at the DP shown in several devices on a log scale. (b) Conductance peak in device 2 at different magnetic fields shows the decrement of the amplitude with increasing B. (c) The conductance peak amplitude increases with increasing temperature. The red dashed lines in the last two panels display fitting of the peak line shape with Eq. 1. (d) No conductance peak at the DP is seen for  $T > T_C$ .

which is close to that extracted from the Andreev curve at  $B=10\text{T}$  as shown in Fig. 4a. These observations – appearance of BCS peaks in the Andreev curve (Fig. 1d) in a QH plateau and excellent agreement with the T dependence predicted by the BCS theory (Fig. 1e) – unambiguously demonstrate the coexistence of QH effect and superconductivity. It is noted that for bulk  $\text{NbSe}_2$ , the critical magnetic field is  $H_{c2} \sim 4\text{-}5\text{T}$ [44], but surface superconductivity ( $H_{c3}$ ) has been reported for up to  $B=7\text{-}8\text{T}$ [45]; the existence of superconductivity at the interface of SLG- $\text{NbSe}_2$  at high magnetic field is thus not unexpected.

We next come to AR. Some evidence for it can be seen from the fact that the conductance at the  $2e^2/h$  plateau is enhanced by  $\sim 15\%$  (Fig.1h) when  $V_{SD}$  is changed from  $-3\text{mV}$ , where no AR is expected (because  $|V_{SD}| > \Delta$ ), to zero, where AR is expected. For an ideal, fully transparent contact, one expects 100% enhancement due to AR; we attribute the smaller enhancement in our system to a non-fully transparent contact. Temperature dependence of conductance enhancement at  $\nu = 2$  is shown in SM Fig.

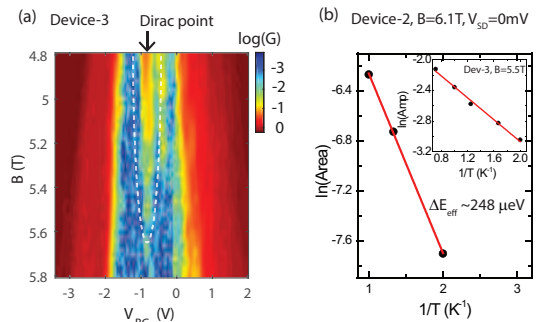


Figure 3. (Color Online) (a) 2D colmap of  $\log(G)$  in device 3 plotted as a function of  $V_{BG}$  and  $B$  showing the presence of the anomalous peak precisely at the DP, which vanishes above  $5.6\text{T}$ . (b) Area of the peak plotted as a function of  $1/T$  showing activated behavior with an effective gap of  $\Delta E_{\text{eff}} \sim 248\mu\text{eV}$ . In the inset, amplitude of conductance peak in device-3 is used to show the activated behaviour, which gives  $\Delta E_{\text{eff}} \sim 150\mu\text{eV}$ .

SI4-5g[33]. Conductance enhancement due to AR can also be seen by comparing the data below and above  $T_C$  shown in SM Fig. SI4-5e[33]. We note that the change in conductance for Andreev curve in Fig. 1f is around 10%. However, the change of conductance was higher  $\sim 25\text{-}30\%$  for device2 in the QH regime (at  $\nu = 2$  plateau) as shown in SM Fig. SI6-8[33]. At  $0\text{T}$  the changes in Andreev curve was around 20% in device1 (SM Fig. SI6-7[33]) and 45-50% in device2 (SM Fig. SI6-8[33]).

Our most important finding is shown in Fig. 2, where a closer inspection of the conductance minimum reveals, completely unexpectedly, an anomalous peak. Further investigation brings out the following properties. First, the peak is seen precisely at the DP. Second, the peak is not seen above  $T_C$  (compare Figs. 2d and 2c). Third, its amplitude decreases with decreasing temperature as well as increasing  $\Delta E_I$ , indicating that the peak is a finite temperature effect. Fig. 3a shows the 2D colmap of  $\log(G)$  plotted as a function of  $V_{BG}$  and  $B$ , which displays the appearance of the peak precisely at the DP and its continuous decrement with increasing  $B$ . Finally, the parameters for which the anomalous peak is observed in device 2 and device 3 are shown by the dashed enclosed areas in the phase diagram in Fig. 4a; for both the devices the highlighted regime where the peak is observed satisfies the condition,  $\Delta E_I < 2\Delta$ .

All of these facts are naturally explained in terms of a conductance peak originating from a new mechanism, namely finite temperature inter-Landau level AR, in which a thermally excited electron in the  $N = 0$  LL band above the  $E_F$  reflects as a hole in the  $N = 0$  LL band below the  $E_F$ , as shown schematically in Fig. 4b. Such a peak is expected to occur (i) precisely at the DP, (ii) at finite temperature but for  $T < T_c$ , and (iii) for  $2\Delta \geq \Delta E_I$ . We mention that  $V_{BG}$  at the DP depends slightly on whether the sweep is up or down, causing two

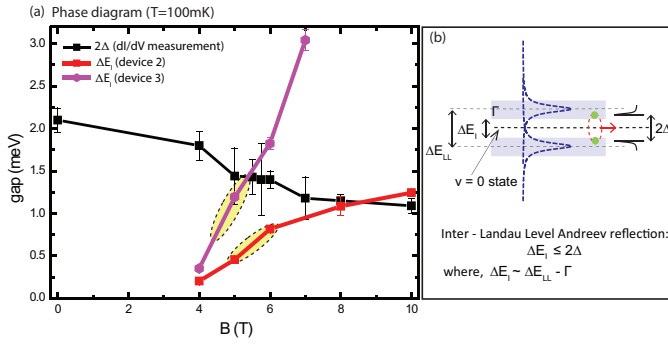


Figure 4. (Color Online) (a) An experimental phase diagram in energy and magnetic field. Filled black squares are the superconducting gaps measured using bias spectroscopy as a function of  $B$ . The filled red squares and filled violet hexagons show the insulating gaps of device-2 and device-3 as a function of  $B$ , where the thick lines are the guide to the eye. The anomalous conductance peak at the DP is observed in the region enclosed by the dashed black ovals. (b) Schematic of inter-Landau level AR process at the DP.

different values in Fig. 2b; in Fig. 3a, all data are for sweep in the up direction, and show that the peak position remains invariant. We also note the presence of certain secondary, sample-specific peaks away from the DP, but their amplitudes are smaller by two to three orders of magnitude.

To see the activated nature of anomalous peak we plot the area under the peak in Fig. 3b for device 2, and fit it to a thermally activated behavior. Fitting the peak height gives a similar gap, as shown for device 3 in the inset of Fig. 3b. Further details regarding the activation nature of the peak for all the devices are shown in SM Sec. SI8 and SI9[33]. Fitting the area in Fig. 3b using  $e^{-\Delta E_{\text{eff}}/2k_B T}$  gives  $\Delta E_{\text{eff}} \sim 0.25$  meV. One may expect  $\Delta E_{\text{eff}}$  to be equal to the  $\Delta E_I$  (mobility gap), but the former is lower by a factor of  $\sim 3$ . This finds a natural explanation by the fact that the temperature dependence of the resistance of SLG shows two distinct  $\Delta E_I$  differing by a factor of  $\sim 3$  (SM Sec. SI5[33]): for example at  $B = 6$ T in device 2 for  $T > 2$ K we have  $\Delta E_I \sim 0.8$ meV, but for  $T < 2$ K we have  $\Delta E_I \sim 0.25$ meV, the latter being essentially in perfect agreement with the gap deduced from the anomalous peak at the DP. Similar results are obtained for device 3 as shown in SM Sec. SI5[33]. Although the existence of the smaller, or ‘soft’ gap around the  $E_F$  in between the LLs at low temperature has been reported in the literature[42, 46–48], its origin is not well understood. We ascribe the ‘soft gap’ below 2K to disorder.

To further confirm the physics of the inter-Landau level AR we have performed extensive numerical calculations, where we consider a system of graphene in the QH regime connected to superconducting graphene. The physics of the  $\nu = 0$  insulator at high  $B$  has been the subject of

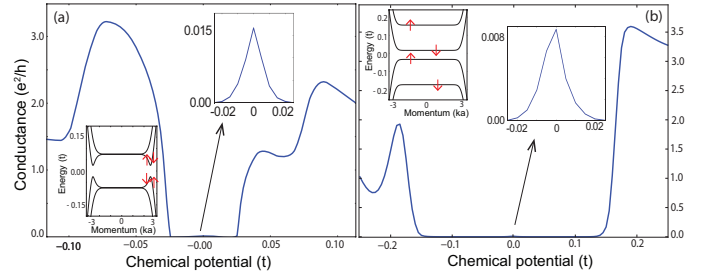


Figure 5. (Color Online) Panel **a** shows numerical results based on canted antiferromagnetic (CAF) model, and the panel **b** for the isospin ferromagnet (IFM) model. The chemical potential is quoted in units of the hopping parameter  $t$ . The band diagram and the peak at the Dirac point are shown as insets.

many studies[37, 39–41, 49, 50] and two most likely models are in terms of a canted antiferromagnet (CAF) or an isospin ferromagnet (IFM)[30, 32], the band diagrams for which are schematically shown in the insets of Figs. 5a and 5b. The insulating gap of the former originates from a splitting of the  $\nu = 0$  LL into Landau bands with chiral edge states, whereas for the latter it results from a coupling between the helical edge states. To keep the discussion general, we consider AR in both models. The calculated conductance as a function of chemical potential ( $E_F$ ) is plotted in Figs. 5a and 5b (SM-theory[33] for the details) for CAF and IFM, respectively. It shows a small conductance peak at the DP arising from inter-Landau level AR (insets of Fig. 5a and 5b). At finite temperatures, the conductance at the DP can be analytically expressed as

$$G = \frac{e^2}{h} \frac{2a}{1 + e^{[\Delta E_I/2 + C(V_{BG} - V_D)]/k_B T}} \quad (1)$$

where  $a$  is the probability of AR and  $C = dE_F/dV_{BG}$ . The experimental peak in Fig. 2c is fitted using the above equation with fitting parameters:  $a=0.35$ ,  $\Delta E_I=0.5$  meV,  $C=0.62$  meV/V for  $T=1$ K and similar fitting is also shown for  $T = 0.75$ K. The fitting parameters are in general agreement with the experimental values (SM-theory[33]).

Before ending, a comment on the physical origin of the observed asymmetry of the Andreev curves (Fig. 1f and SM Sec. SI6[33]) is in order.  $dI/dV$  depends on the joint density of states (DOS) of the two materials. Typically, a normal metal has large and essentially constant DOS whereas the quasiparticle DOS of the superconductor is symmetric around zero bias, producing a symmetric Andreev curve. The density of states in a QH edge, in contrast, is complicated in real materials and can be energy dependent, thus producing asymmetric Andreev curves[16, 51–53]. We also note that due to the presence of the superconductor, the skipping orbits at the interface alternate between electron and hole-type

orbits, whose centers are in general slightly offset (Fig. 1a bottom)[22, 24], which results in an interference pattern. The fingerprints of the interference pattern can be seen as quasiperiodic conductance oscillations on the QH plateau as a function of the chemical potential (Fig. 1h and SM Sec. S110[33]). We refer the reader to previous literatures[16, 22, 24, 51–55] and the SM[33] for details.

In conclusion, our primary accomplishment is an unambiguous demonstration of AR in graphene quantum Hall effect, which manifests most dramatically through an anomalous finite-temperature conductance peak at the Dirac point. By a combination of experimental and theoretical studies, we have confirmed its origin as thermally induced inter-Landau level AR.

We thank Subhro Bhattacharjee, Tanmoy Das, H.R. Krishnamurthy, Subroto Mukerjee, Sumathi Rao, Sambuddha Sanyal, Ruchi Sexena, Vijay Shenoy, and Abhiram Soori for useful discussions. The authors acknowledge device fabrication and characterization facilities in CeNSE, IISc, Bangalore. AD thanks Department of Science and Technology (DST), Government of India, under Grants no. DSTO1470 and DSTO1597. We also acknowledge the support by the US Department of Energy under Grant No. DE-SC0005042 (JKJ) and National Key R&D Program of China (Grant No. 2016YFA0401003) and NSFC (Grant No.11674114 (XL)).

---

\* anindya@iisc.ac.in

- [1] L. Fu and C. L. Kane, Physical review letters **100**, 096407 (2008).
- [2] R. M. Lutchyn, J. D. Sau, and S. D. Sarma, Physical review letters **105**, 077001 (2010).
- [3] Y. Oreg, G. Refael, and F. von Oppen, Physical review letters **105**, 177002 (2010).
- [4] V. Mourik, K. Zuo, S. M. Frolov, S. Plissard, E. Bakkers, and L. Kouwenhoven, Science **336**, 1003 (2012).
- [5] A. Das, Y. Ronen, Y. Most, Y. Oreg, M. Heiblum, and H. Shtrikman, Nature Physics **8**, 887 (2012).
- [6] R. S. Mong, D. J. Clarke, J. Alicea, N. H. Lindner, P. Fendley, C. Nayak, Y. Oreg, A. Stern, E. Berg, K. Shtengel, *et al.*, Physical Review X **4**, 011036 (2014).
- [7] J. Alicea and P. Fendley, Annual Review of Condensed Matter Physics **7**, 119 (2016).
- [8] D. J. Clarke, J. Alicea, and K. Shtengel, Nature Physics **10**, 877 (2014).
- [9] K. S. Novoselov, A. K. Geim, S. V. Morozov, D. Jiang, Y. Zhang, S. V. Dubonos, I. V. Grigorieva, and A. A. Firsov, science **306**, 666 (2004).
- [10] L. Wang, I. Meric, P. Huang, Q. Gao, Y. Gao, H. Tran, T. Taniguchi, K. Watanabe, L. Campos, D. Muller, *et al.*, Science **342**, 614 (2013).
- [11] K. S. Kim, Y. Zhao, H. Jang, S. Y. Lee, J. M. Kim, K. S. Kim, J.-H. Ahn, P. Kim, J.-Y. Choi, and B. H. Hong, nature **457**, 706 (2009).
- [12] C. Beenakker, Physical review letters **97**, 067007 (2006).
- [13] C. Beenakker, Reviews of Modern Physics **80**, 1337 (2008).
- [14] V. E. Calado, S. Goswami, G. Nanda, M. Diez, A. R. Akhmerov, K. Watanabe, T. Taniguchi, T. M. Klapwijk, and L. M. Vandersypen, Nature nanotechnology **10**, 761 (2015).
- [15] M. T. Allen, O. Shtanko, I. C. Fulga, A. Akhmerov, K. Watanabe, T. Taniguchi, P. Jarillo-Herrero, L. S. Levitov, and A. Yacoby, Nature Physics **12**, 128 (2016).
- [16] D. Efetov, L. Wang, C. Handschin, K. Efetov, J. Shuang, R. Cava, T. Taniguchi, K. Watanabe, J. Hone, C. Dean, *et al.*, Nature Physics (2015).
- [17] M. R. Sahu, P. Raychaudhuri, and A. Das, Physical Review B **94**, 235451 (2016).
- [18] Z. Han, A. Allain, H. Arjmandi-Tash, K. Tikhonov, M. Feigelman, B. Sacepe, and V. Bouchiat, Nature Physics **10**, 380 (2014).
- [19] A. Soori, M. R. Sahu, A. Das, and S. Mukerjee, arXiv preprint arXiv:1801.00620 (2018).
- [20] W. Bishara and C. Nayak, Physical review letters **99**, 066401 (2007).
- [21] C. Nayak, S. H. Simon, A. Stern, M. Freedman, and S. D. Sarma, Reviews of Modern Physics **80**, 1083 (2008).
- [22] H. Hoppe, U. Zülicke, and G. Schön, Physical review letters **84**, 1804 (2000).
- [23] M. P. Fisher, Physical Review B **49**, 14550 (1994).
- [24] F. Giazotto, M. Governale, U. Zülicke, and F. Beltram, Phys. Rev. B **72**, 054518 (2005).
- [25] A. Akhmerov and C. Beenakker, Physical review letters **98**, 157003 (2007).
- [26] F. Amet, C. T. Ke, I. V. Borzenets, J. Wang, K. Watanabe, T. Taniguchi, R. S. Deacon, M. Yamamoto, Y. Bomze, S. Tarucha, *et al.*, Science **352**, 966 (2016).
- [27] M. B. Shalom, M. Zhu, V. Falko, A. Mishchenko, A. Kretinin, K. Novoselov, C. Woods, K. Watanabe, T. Taniguchi, A. Geim, *et al.*, Nature Physics **12**, 318 (2016).
- [28] P. Rickhaus, M. Weiss, L. Marot, and C. Schonenberger, Nano Letters **12**, 1942 (2012).
- [29] G.-H. Lee, K.-F. Huang, D. K. Efetov, D. S. Wei, S. Hart, T. Taniguchi, K. Watanabe, A. Yacoby, and P. Kim, Nature Physics (2017).
- [30] D. A. Abanin, P. A. Lee, and L. S. Levitov, Physical review letters **96**, 176803 (2006).
- [31] P. Tikhonov, E. Shimshoni, H. Fertig, and G. Murthy, Physical Review B **93**, 115137 (2016).
- [32] M. Kharitonov, “Edge excitations of the canted antiferromagnetic phase of the  $\nu=0$  quantum hall state in graphene: A simplified analysis,” (2012).
- [33] See supplemental material at [URL will be inserted by APS] for additional data on device fabrication and characterization, QH response, Andreev curves and numerical simulation of Andreev reflection in QH regime.
- [34] J. Xue, J. Sanchez-Yamagishi, D. Bulmash, P. Jacquod, A. Deshpande, K. Watanabe, T. Taniguchi, P. Jarillo-Herrero, and B. J. LeRoy, Nat Mater **10**, 282 (2011).
- [35] X. Hong, K. Zou, and J. Zhu, Physical Review B **80**, 241415 (2009).
- [36] A. F. Young, C. R. Dean, L. Wang, H. Ren, P. Cadden-Zimansky, K. Watanabe, T. Taniguchi, J. Hone, K. L. Shepard, and P. Kim, Nature Physics **8**, 550 (2012).
- [37] Y. Zhang, Z. Jiang, J. Small, M. Purewal, Y.-W. Tan, M. Fazlollahi, J. Chudow, J. Jaszczak, H. Stormer, and P. Kim, Physical review letters **96**, 136806 (2006).
- [38] Z. Jiang, Y. Zhang, H. Stormer, and P. Kim, Physical

- review letters **99**, 106802 (2007).
- [39] J. G. Checkelsky, L. Li, and N. Ong, Physical review letters **100**, 206801 (2008).
- [40] X. Du, I. Skachko, F. Duerr, A. Luican, and E. Y. Andrei, Nature **462**, 192 (2009).
- [41] K. I. Bolotin, F. Ghahari, M. D. Shulman, H. L. Stormer, and P. Kim, Nature **462**, 196 (2009).
- [42] A. Giesbers, U. Zeitler, M. Katsnelson, L. Ponomarenko, T. Mohiuddin, and J. Maan, Physical review letters **99**, 206803 (2007).
- [43] J. Rodrigo and S. Vieira, Physica C: Superconductivity **404**, 306 (2004).
- [44] X. Xi, Z. Wang, W. Zhao, J.-H. Park, K. T. Law, H. Berger, L. Forró, J. Shan, and K. F. Mak, Nature Physics (2015).
- [45] G. D'anna, P. Gammel, A. Ramirez, U. Yaron, C. Oglesby, E. Bucher, and D. Bishop, Physical Review B **54**, 6583 (1996).
- [46] S. Koch, R. Haug, K. Von Klitzing, and K. Ploog, Semiconductor science and technology **10**, 209 (1995).
- [47] A. Efros and B. Shklovskii, Journal of Physics C: Solid State Physics **8**, L49 (1975).
- [48] K. Bennaceur, P. Jacques, F. Portier, P. Roche, and D. Glattli, Physical Review B **86**, 085433 (2012).
- [49] A. F. Young, J. Sanchez-Yamagishi, B. Hunt, S. H. Choi, K. Watanabe, T. Taniguchi, R. Ashoori, and P. Jarillo-Herrero, Nature **505**, 528 (2014).
- [50] Y. J. Song, A. F. Otte, Y. Kuk, Y. Hu, D. B. Torrance, P. N. First, W. A. de Heer, H. Min, S. Adam, M. D. Stiles, *et al.*, Nature **467**, 185 (2010).
- [51] K. Komatsu, C. Li, S. Autier-Laurent, H. Bouchiat, and S. Guéron, Physical Review B **86**, 115412 (2012).
- [52] G.-H. Park, M. Kim, K. Watanabe, T. Taniguchi, and H.-J. Lee, Scientific reports **7**, 10953 (2017).
- [53] H. Takayanagi and T. Akazaki, Physica B: Condensed Matter **249**, 462 (1998).
- [54] A. Morpurgo, J. Kong, C. Marcus, and H. Dai, Science **286**, 263 (1999).
- [55] A. Finck, D. Van Harlingen, P. Mohseni, K. Jung, and X. Li, Physical review letters **110**, 126406 (2013).